Current Biology, Volume *22*

Supplemental Information

A PHABULOSA/Cytokinin Feedback Loop Controls Root Growth in *Arabidopsis*

Raffaele Dello Ioio, Carla Galinha, Alexander G. Fletcher, Stephen P. Grigg, Attila Molnar, Viola Willemsen, Ben Scheres, Sabrina Sabatini, David Baulcombe, Philip K. Maini, and Miltos Tsiantis

Supplemental Inventory

Supplemental Figures

Supplemental Experimental Procedures

Supplemental References

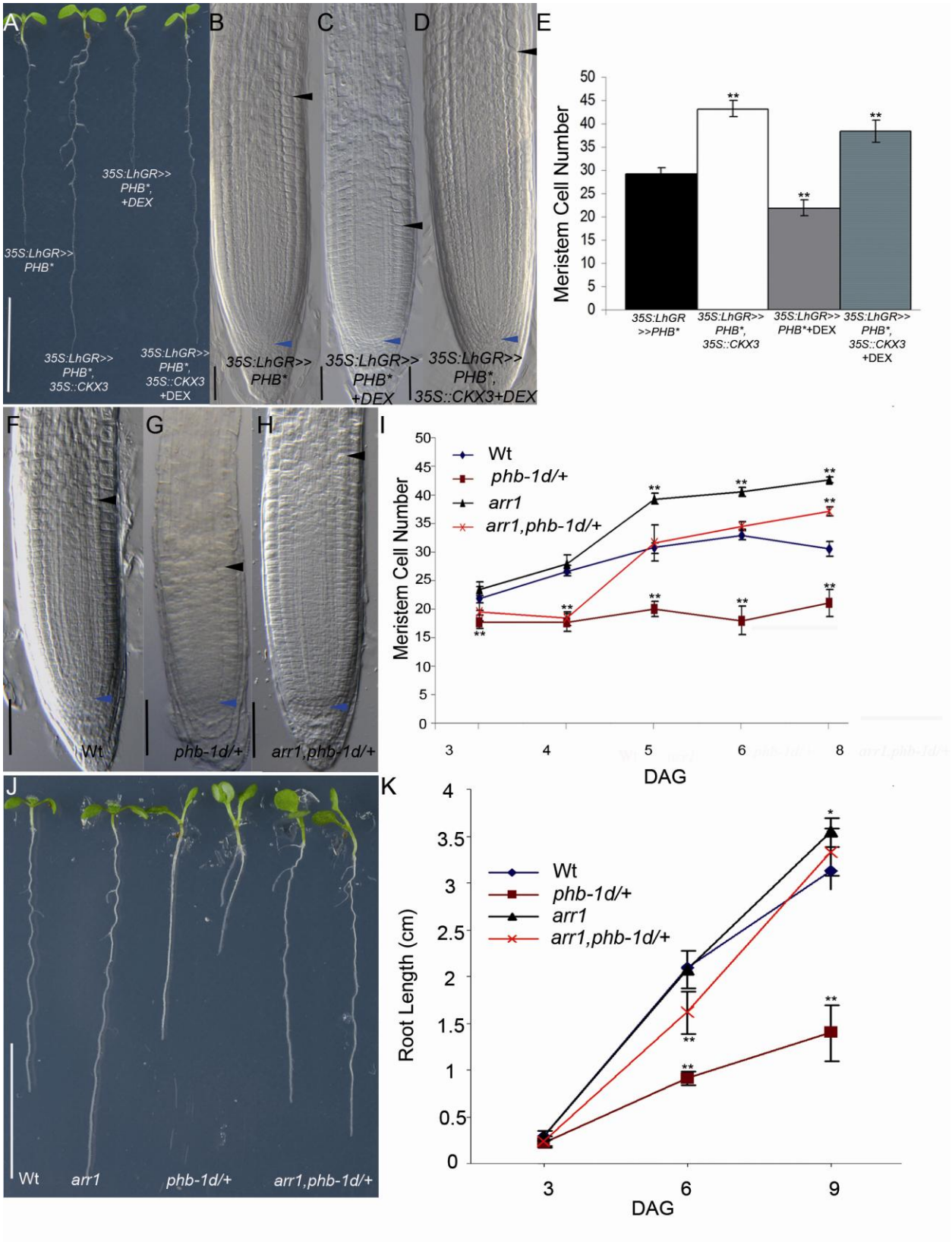
A
B
C
D
E
35S:LhGR>>
PHB*,
+DEX
35S:LhGR>>
PHB*
35S:LhGR>>
PHB*,
35S::CKX3
35S:LhGR>>
PHB*,
35S::CKX3
+DEX
35S:LhGR>>
PHB*
35S:LhGR>>
PHB*
+DEX
35S:LhGR>>
PHB*,
35S::CKX3+DEX
Meristem Cell Number
35S:LhGR
>>PHB*
35S:LhGR>>
PHB*,
35S::CKX3
35S:LhGR>>
PHB*+DEX
35S:LhGR>>
PHB*,
35S::CKX3
+DEX
F
G
H
I
Wt
phb-1d/+
arr1,phb-1d/+
Meristem Cell Number
DAG
Wt
phb-1d/+
arr1
arr1,phb-1d/+
J
K
Wt
arr1
phb-1d/+
arr1,phb-1d/+
Root Length (cm)
DAG
Wt
phb-1d/+
arr1
arr1,phb-1d/+

Figure S1.

Figure S1. PHB and PHV Regulate CK Activity in the Root (Related to Figure 1)

(A) 7-DAG seedlings (from left to right): *35S:LhGR>>PHB**, *35S:LhGR>>PHB*,35S::CKX3*, *35S:LhGR>>PHB** germinated on 50 μM DEX and 3*5S:LhGR>>PHB*,35S::CKX3* germinated on 50 μM DEX. Scale bar: 1 cm.

(B-D) Root meristem of 7-DAG *35S:LhGR>>PHB** (B), *35S:LhGR>>PHB** germinated on 50 μM dexamethasone (DEX) (C) and 3*5S:LhGR>>PHB*,35S::CKX3* germinated on 50 μM DEX (D). Blue and black arrowheads indicate respectively the stem cell and the TZ of the cortex. Scale bars: 50 μm.

(E) Number of cortex cells in the root meristem at 7-DAG of *35S:LhGR>>PHB** and *35S:LhGR>>PHB*,35S::CKX3* plants germinated on control medium and on 50 μM DEX. Root meristem length was measured as the number of cortex cells between the cortex stem cell (blue arrowhead) and the first elongated cortex cell (black arrowhead). Error Bars, SD.

(F-H) 5-DAG root meristem of WT (F), *phb-1d/+* (G) and *arr1-4,phb-1d/+* (H). Arrowheads indicate root meristem borders. Meristem borders are depicted as in (B-D). Scale bars: 50μm.

(I) Number of cortex cells in the root meristem of WT, *phb-1d/+*, *arr1-4* and *phb-1d/+,arr1-4* over time. Note that *arr1,phb-1d/+* root meristem cell number is the same of the WT only from 5 DAG, coinciding with the timing of expression of *ARR1* [1]. Error bars, SD.

(J) 10-DAG (from left to right) WT, *arr1-4*, *phb1-d/+* and *arr1-4,phb-1d/+* seedlings. Scale bar: 1 cm.

(K) Root length over time of *phb-1d/+*, *arr1-4* and *arr1-4,phb-1d/+* in comparison to WT. Error bars, SD.

*$p < 0.05$, **$p < 0.01$, Student's t test.

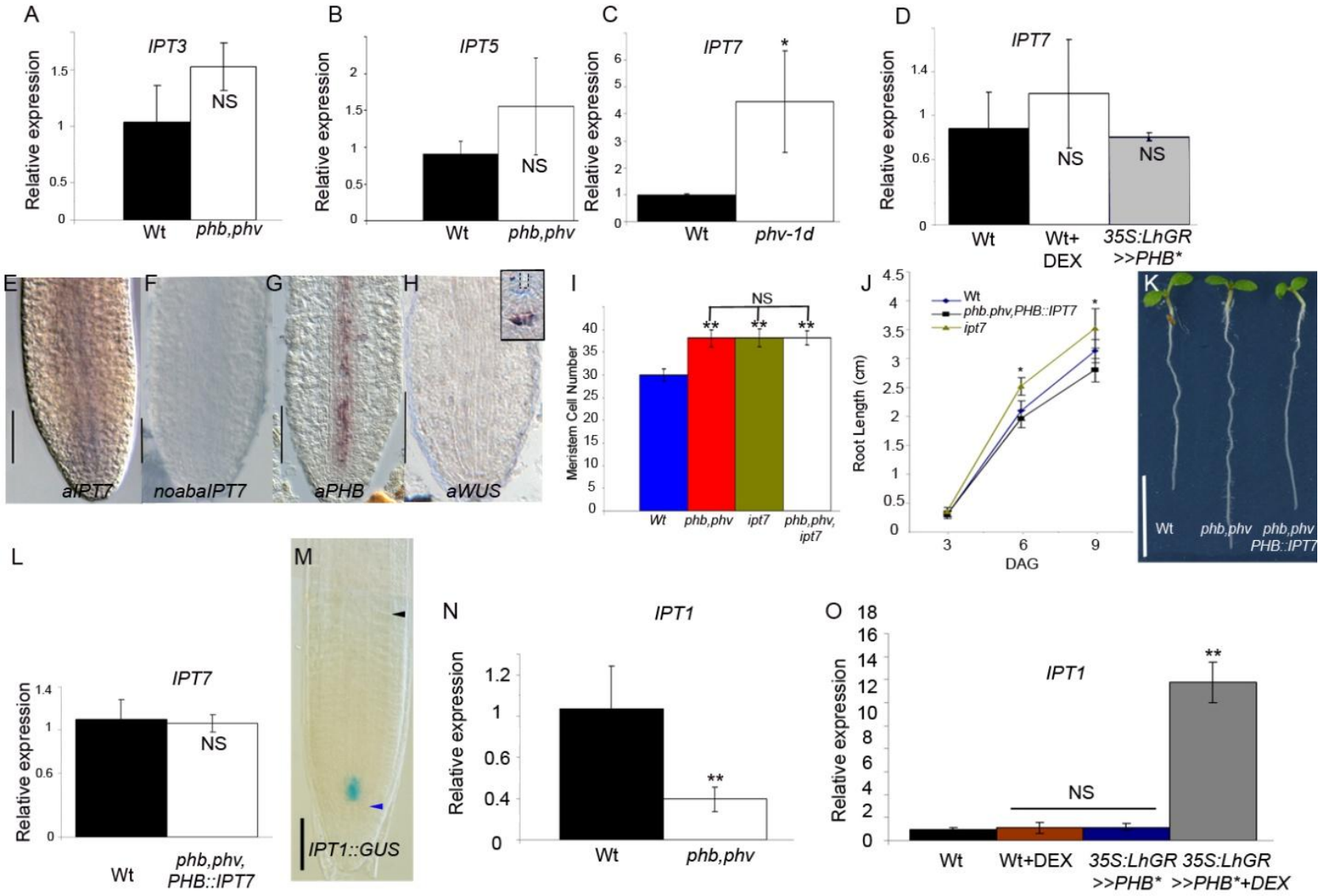
A
IPT3
Relative expression
NS
Wt
phb,phv
B
IPT5
Relative expression
NS
Wt
phb,phv
C
IPT7
*
Relative expression
Wt
phv-1d
D
IPT7
Relative expression
NS
NS
Wt
Wt+ DEX
35S:LhGR >>PHB*
E
F
G
H
aIPT7
noabaIPT7
aPHB
aWUS
I
NS
**
**
**
Meristem Cell Number
Wt
phb,phv
ipt7
phb,phv, ipt7
J
Wt
phb.phv,PHB::IPT7
ipt7
Root Length (cm)
DAG
K
Wt
phb,phv
phb,phv PHB::IPT7
L
IPT7
Relative expression
NS
Wt
phb,phv, PHB::IPT7
M
IPT1::GUS
N
IPT1
Relative expression
**
Wt
phb,phv
O
IPT1
Relative expression
**
NS
Wt
Wt+DEX
35S:LhGR >>PHB*
35S:LhGR >>PHB*+DEX

Figure S2.

Figure S2. PHB Regulates *IPT7* and *IPT1* Expression (Related to Figure 2)

(A and B) Relative abundance of *IPT3* (A) and *IPT5* (B) mRNA in *phb-13,phv-11*. Error bars, SD, n=3. Note that neither *IPT3* nor *IPT5* expression was altered in *phb,phv* mutants.

(C) Relative abundance of *IPT7* mRNA in *phv-1d* (C). *IPT7* mRNA levels are strongly enhanced in *phv-1d* mutants. Error bars, SD, n=3.

(D) Relative expression of *IPT7* mRNA in WT, WT treated with DEX (50 μM) and untreated *35S:LhGR>>PHB** plants. The relative expression of *IPT7* does not change after DEX application and in untreated *35S:LhGR>>PHB** in comparison to the WT. Error bars, SD, n=3.

(E and F) mRNA in situ hybridization with *IPT7* (E) and *IPT7* no antibody control (F) specific antisense probes in WT bent cotyledon stage embryos.

(G and H) mRNA in situ hybridization with *PHB* (G) and *WUS* (H) specific antisense probes in WT bent cotyledon stage embryos. WUS antisense probe was used as background control for the root, because this gene is expressed only in the shoot apical meristem (box in (H)). The timing of staining of the two probes was the same. (E) and (G) show that the expression of *PHB* and *IPT7* overlaps in the root vascular tissue. Scale Bars: 50 μm.

(I) 5-DAG root meristem cell number of WT, *phb-13,phv-11*, *ipt7-1* and *phb-13,phv-11,ipt7-1*. Error bars, SD. Note that *phb-13,phv-11*, *ipt7-1* and *phb-13,phv-11,ipt7-1* mutants have similar root meristem size and thus, the difference between their meristem sizes is statistically not significant (NS).

(J) Root length over time of *ipt7-1*, *phb,phv,PHB::IPT7* and WT. Error Bars, SD.

(K) 5-DAG (from left to right) WT, *phb-13,phv-11* and *phb-13,phv-11,PHB::IPT7* seedlings. Scale bar: 1 cm.

(L) Relative expression of *IPT7* mRNA in *phb-13,phv-11,PHB::IPT7* in comparison to the WT. *IPT7* mRNA levels are similar to the WT. Error bars, SD, n=3.

(M) *IPT1::GUS* expression in 4-DAG root meristems of WT. Scale Bar: 50 μm. Blue and black arrowheads indicate respectively the cortex stem cell and the cortex TZ.

(N and O) Relative expression of *IPT1* mRNA in *phb,phv* in comparison to WT plants (N) and in WT, WT treated with DEX (50 μM 4 h), untreated *35S:LhGR>>PHB** and DEX treated *35S:LhGR>>PHB** plants (O). Error bars, SD, n=3.

*$p < 0.05$, **$p < 0.01$, NS, not significant, Student's t test.

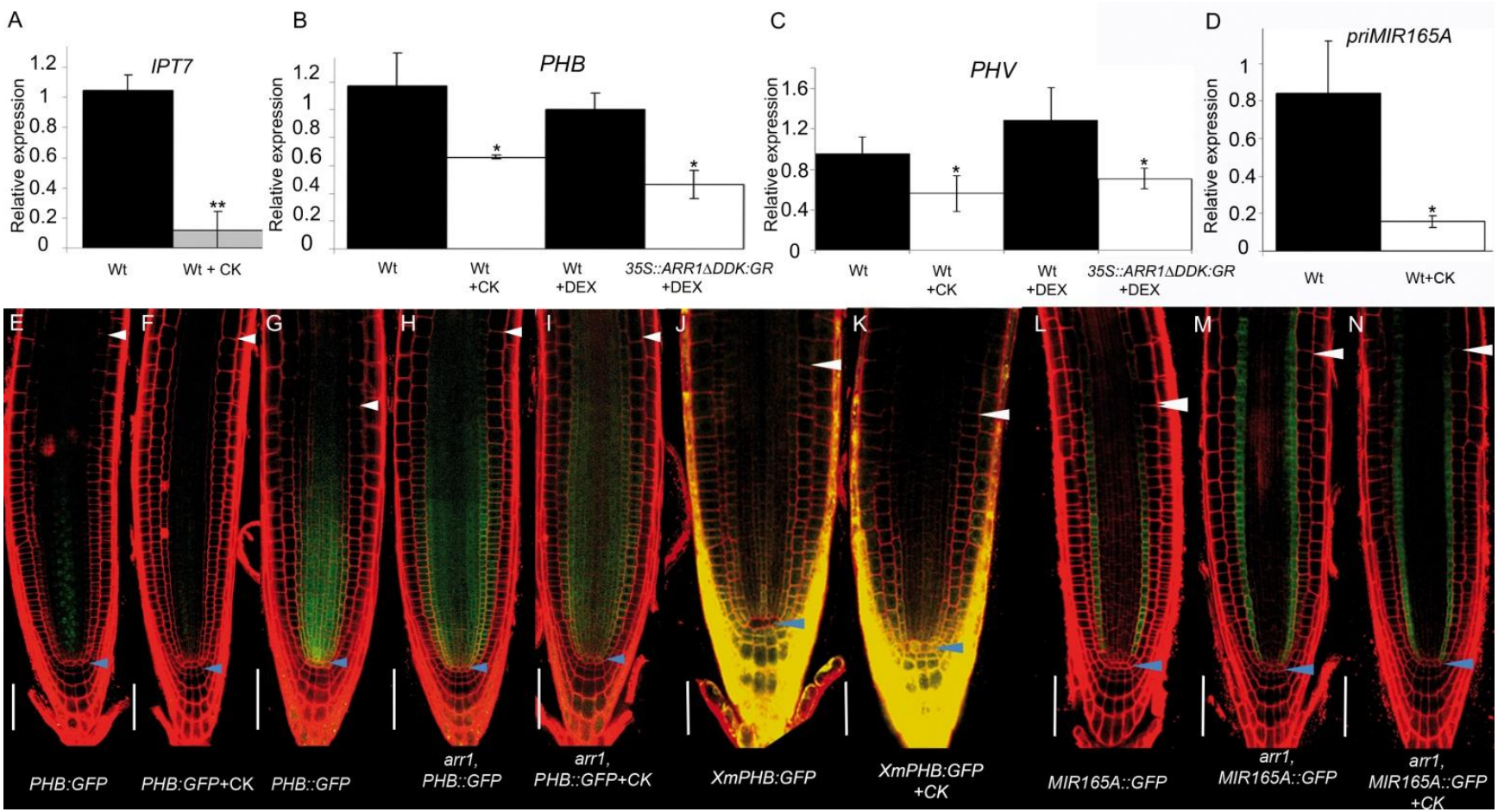

Figure S3. CK Negatively Regulates *IPT7, PHB, PHV,* and *MIR165A* Expression (Related to Figure 3)

(A) Relative expression of *IPT7* mRNA in WT plants treated with CK (6 hours, 5 μM *trans*-zeatin). Error bars, SD, n=3.

(B) Relative expression of *PHB* mRNA in WT treated with CK (6 hours, 5 μM *trans*-zeatin), WT treated with 50 μM DEX and *35S::ARR1ΔDDK:GR* treated with 50 μM DEX. Error bars, SD, n=3.

(C) Relative expression of *PHV* mRNA in WT treated with CK (6 hours, 5 μM *trans*-zeatin), WT treated with 50 μM DEX and *35S::ARR1ΔDDK:GR* treated with 50 μM DEX. Error bars, SD, n=3.

(D) Relative expression of *priMIR165A* in WT and in WT after CK treatment (6 hours, 5 μM *trans*-zeatin). Error Bars, SD, n=3.

(E and F) Expression of the translational reporter *PHB:GFP* in 5-DAG WT root meristems in control medium (E) and after CK treatment (5 μM *trans*-zeatin for 6 hours) (F). Note that CK treatment strongly reduces *PHB:GFP* expression.

(G-I) Expression of the transcriptional reporter *PHB::GFP* in 5-DAG meristems of WT (G), *arr1-3* (H) and *arr1-3* after CK treatment (16 hours, 5 μM *trans*-zeatin) (I). In *arr1* mutants, *PHB::GFP* is ectopically expressed in the TZ (white arrowhead) and does not decrease after CK.

(J and K) Root meristem of 5-DAG *sde1-1* plants expressing a mutated control version of the mir165/6 sensor (*XmPHB:GFP*) in control (J) and CK treated (16 h, 5 μM *trans*-zeatin) (K) plants.

(L-N) 5-DAG root meristem of plants expressing *MIR165A::GFP* in WT (L), *arr1-4* (M) and *arr1-4* after CK treatment (16 hours, 5 μM *trans*-zeatin) (N). *MIR165A* expression is stronger at the TZ (white arrowhead) in *arr1* mutants and does not decrease after CK application.

Blue arrowheads indicate the cortex stem cell and white arrowheads indicate the cortex TZ. Scale bars: 50 μm.

*$p < 0.05$, **$p < 0.01$, Student's t test.

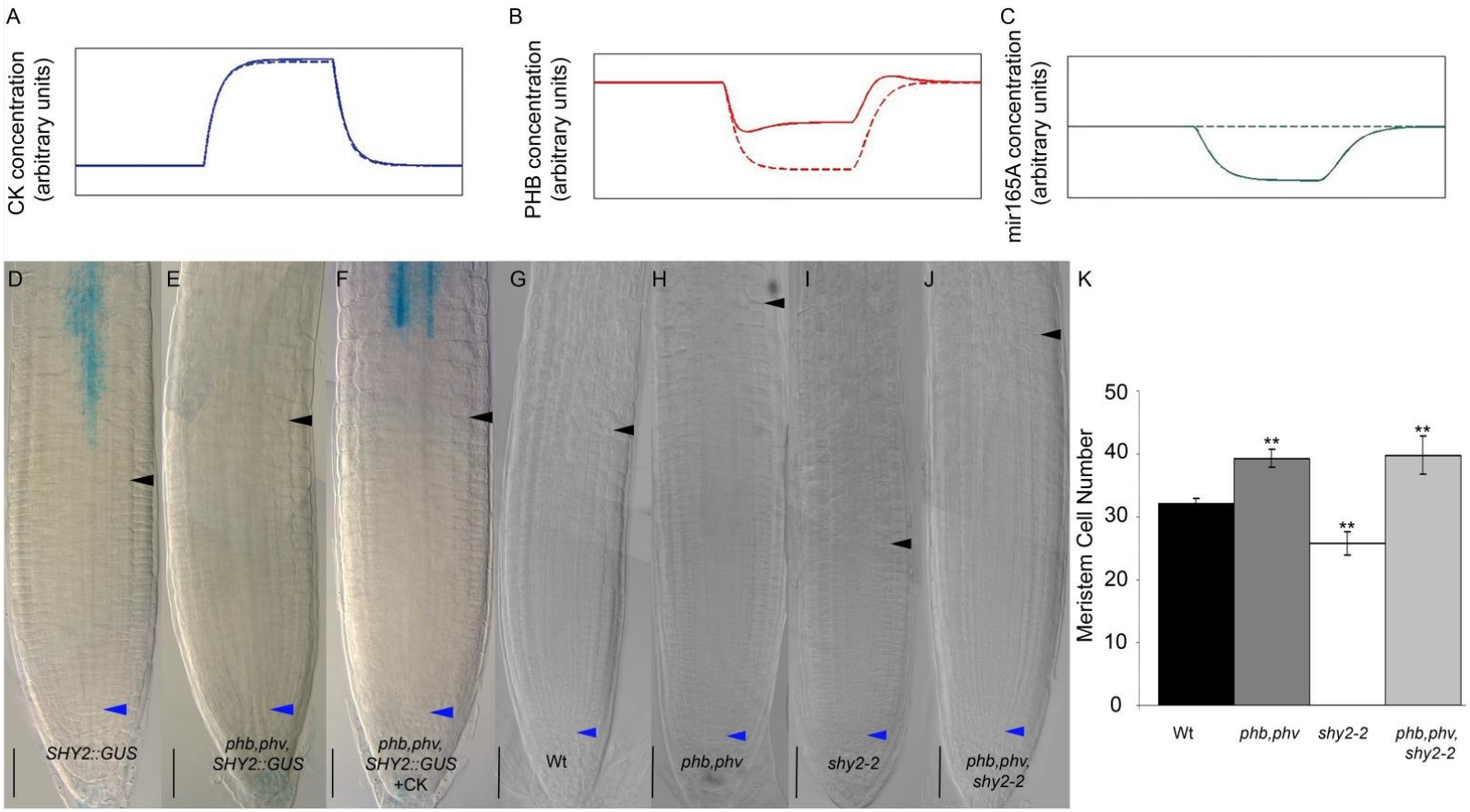

Figure S4. Regulatory Interplay between PHB and CK activity (Related to Figure 4)

(A-C) Simulation of the dynamic behaviour of CK (A), PHB (B) and mir165/6 (C) levels in response to a temporary increase in the rate of CK synthesis. Details of the computational model used are provided in the computational simulations on page 15. The model parameter α_1 (the baseline rate of CK synthesis) is stepped up from 0 to 1 then back to 0. Time is in arbitrary units. Solid lines: full system. Dashed lines: simple system with no repression of mir165/6 by CK and same steady-state levels in the absence of CK synthesis. The simulation output shows that this component of the regulatory circuit accelerates the PHB response, and results in an elevated equilibrium level, in response to a temporary increase in the rate of CK synthesis designed to mimic a small fluctuation due to environmental changes.

(D-F) *SHY2::GUS* expression in 5-DAG root meristems of WT (D), *phb-13,phv-11* (E) and CK-treated *phb-13,phv-11* (2 hours, 5 μM *trans*-zeatin) (F) plants. *SHY2* expression is strongly reduced in *phb,phv* background in comparison to the WT and is increased by CK application.

(G-J) 5-DAG root meristem of WT (G), *phb-6,phv-5* (H), *shy2-2* (I) and *shy2-2,phb,phv* (J). Blue and black arrowheads indicate respectively the stem cell and the TZ of the cortex. Scale bars: 50 μm.

(K) Meristem length of WT, *phb-6,phv-5*, *shy2-2* and *phb-6,phv-5,shy2-2* at 5 DAG. Error bars: SD.

**$p < 0.01$, Student's t test.

Supplemental Experimental Procedures

Materials and Methods

Plant Materials

Genotype	Description	References
phb-1d	Strong microRNA-insensitive dominant allele of *phb*. Original mutation in L*er* crossed 5 times to Col-0 WT. These plants show a similar phenotype to *phb-1d* in Ler ecotype background: trumpet leaves and short root. Donated by Scott Poethig and Stewart Gilmore.	[8]
phv-1d	Strong microRNA-insensitive dominant allele of *phv,* (Ler).	[8]
phb-13,phv-11	Double loss-of-function mutant plants of *PHB* and *PHV*, (Col-0).	[14]
phb-6,phv-5	Double loss-of-function mutant plants of *PHB* and *PHV* (Ler).	[14]
arr1-3	Loss of function mutant plants of *ARR1* (Col-0).	[1]
arr1-4	Loss of function mutant plants of *ARR1* (Col-0).	[1]
ipt7-1	Loss of function mutant plants of *IPT7*,SALK institute (Col-0).	SALK_001940
ipt7-2	Loss of function mutant plants of *IPT7*, Col-0, JIC SM lines.	N104591
shy2-2	Dominant allele of *shy2* (Ler).	[1]
35S::ARR1ΔDDK:GR	Dominant DEX inducible version of *ARR1* driven by the 35S promoter (Col-0).	[5]
35S::IPT	Plants harbouring the bacterial *IPT* gene driven by 35S promoter, provided by NASC (Col-0)	N117
*35S:LhGR>>PHB**	Two-component inducible dominant miR insensitive version of PHB. DEX induction causes a phenotype similar to *phb-1d. 35S:LhGR>>PHB** was constructed as follows: *PHB** was amplified from PHB-G202G synonymous mutant cDNA with the primers PHBcdnaXmaF (GACCCGGGATGATGATGGTCCATTCG) and PHBcdnaBamR (CAGGATCCTCAAACGAACGACC) and inserted into *10OP-BJ36.* The NotI cassette containing 10OP::PHB* was inserted in *pMLBART*. This construct was transformed by floral dip into plants harbouring *LhGR* driven by 35S promoter (Col-0). On the basis of previous work we estimated that 4 hours of DEX treatment would be an appropriate time frame for a robust induction of PHB* and genes activated by PHB in a *35S:LhGR>>PHB** two component system, where DEX mediated activation of the synthetic LhGR transcription factor precedes transcriptional activation of the gene of interest-in this case PHB*.	[SR1, 15, SR2]
PHB:GFP*	Translational reporter of a dominant version of *PHB* (*PHB**) fused to the GFP and driven by 2.8 Kb of *PHB* promoter. *PHB::PHB*:GFP* was constructed as follows: The 35S promoter in the vector pEGAD was replaced with a 2.8 kb pPHB fragment amplified with the primers PHBproSacF (CAGAGCTGCCAATGGCGGAAAATGACACC) and PHBproAgeR (GAACCGGTAGCTCAAAGTCAGAAATAGG). *PHB** and *PHB* cDNA were inserted in the MCS in frame with the eGFP gene. This construct was transformed into WT Col-0 plants by floral dip. The obtained lines resemble *phb-1d* mutants.	[SR2]

PHB::IPT7, phb-13,phv-11	*phb-13,phv11* mutant plants harbouring *IPT7* cDNA driven by 2.8 *PHB* promoter. *PHB::IPT7* lines were obtained as follows: *IPT7* cDNA was amplified by cDNA with the following primers ipt7fwcdna (ATGAAGTTCTCAATCTCATCA) and ipt7revcdna (TCATATCATATTGTGGGCTC). The amplified fragment was inserted in pGEMT-easy vector (Promega), digested with EcoRI and filled to blunt with T4 DNA polymerase (NEB). The *IPT7* fragment was then inserted in *PHB-pEGAD* substituting the eGFP with *IPT7*. *phb-13,phv-11* plants were then transformed by floral dip. In this line IPT7 mRNA abundance is comparable to WT (S2C).	[SR2]
RCH2::CKX1	Col plants harbouring the *CKX1* gene under the control of the TZ specific *RCH2* promoter.	[1]
35S::CKX3	Col plants harbouring *CKX3* gene under the control of *35S.*	[SR3]
J2341	Promoter trap line marking the stem cells (Col-0).	[1]
CYCB1:GUS	Reporter line for cell division activity (Col-0).	[SR4]
QC46::YFP	Quiescent Center (QC) activity marker (Col-0).	[SR5]
QC25::CFP	QC activity marker (Col-0).	[SR5]
RCH1::GFP	Meristem activity marker (Col-0)	[1]
PHB::GFP	Transcriptional reporter of *PHB* (Col-0).	[12]
MIR165A::GFP	Transcriptional reporter of *MIR165A* (Col-0).	[12]
PHB:GFP	Translational reporter of *PHB* (Col-0).	[13]
ARR5::GUS	CK activity reporter (Col-0).	[16]
TCS::GFP	CK activity reporter (Col-0).	[17]
XPHB:mGFP	Sensor for mir165/6 activity. *XPHB:mGFP* was constructed as follows: The mir165/6 target sequence of PHB (ttgggatgaagcctggtccgg) was cloned in frame with mGFP under the control of the 35S promoter in pGREENII-0229 vector. To prevent silencing the constructs were transformed in C24 *sde1-1* (*RDR6* loss of function) background.	[SR2, SR6]
XmPHB:mGFP	*XmPHB:mGFP* was constructed as follows: The mutated mir165/6 target sequence of PHB (ttgggatgaagcctgatccgg) was cloned in frame with mGFP under the control of the 35S promoter in pGREENII-0229 vector. To prevent silencing the constructs were transformed in C24 *sde1-1* (*RDR6* loss of function) background.	[SR2, SR6]
SHY2::GUS	Transcriptional reporter of *SHY2* (Col-0).	[5]
IPT1::GUS	Transcriptional reporter of *IPT1* (Col-0).	[21]

Growth Conditions

Arabidopsis seedlings were grown in a 16 hours light/8 hours dark cycle at 18-25 °C on 0.5 x MS with 1% sucrose.

Root length and meristem size analysis have been performed as described in [1]. For each experiment, a minimum of 40 plants were analyzed.

qRT-PCR

Total RNA from 5-DAG roots was extracted using the Nucleospin RNA Kit (Machery and Nagel), and the first strand cDNA was synthesized using the SuperScript® *VILO*™ cDNA Synthesis Kit (Invitrogen). Quantitative RT-PCR analysis was conducted using the following gene-specific primer pairs: qRTPHBfw and qRTPHBrev [12], qRTIPT7fw and qRTIPT7rev

[SR7], qpriMIR165Afw andqpriMIR165Arev [12], qRTIPT3fw and qRTIPT3rev [SR7], qRTIPT5fw and qRTIPT5rev [SR7], qRT IPT1fw and qRTIPT1rev [SR8], qRTPHVfw and qRTPHVrev [12], OTCfw and OTCrev [SR7]. Real time PCR amplification was performed using the double-strand DNA-specific dye SYBR Green (Applied Biosystem) in a 7300 Real Time PCR System (Applied Biosystems). Experiments were performed in triplicate from two independent root tissue RNA extractions. Relative expression was normalized to *ORNITHINE TRANSCARBAMILASE* (*OTC*) control.

Microscopy

Confocal laser scanning imaging was performed on 5-DAG seedlings mounted in propidium iodide (25 μg/ml). Images were taken with a Zeiss 510 Meta microscope.

DIC microscopy was performed on roots mounted in cloral hydrate:glycerol:water (8:2:3) and viewed using an Olympus BX50.

GUS Analysis

GUS activity was detected using 1 mg/ml 5-bromo-4-chloro-3-indolyl-β-D-glucuronic acid (Molecular Probes) supplemented with ferrocyanide and ferricyanide salts (0.5 mM).

Fluorescence Quantification

The quantification of GFP fluorescence in the transgenic lines analyzed was performed as in [6]. The GFP signal intensity of each sample was normalized to the GFP signal intensity in the WT. For each experiment approximately 20 images/seedlings were examined.

ChIP

ChIP was performed on 12 DAG seedlings of *PHB*:GFP* plants as described in [SR9] with some modifications. 1 gram of seedlings were fixed in Fixative Solution (0.4M Sucrose, 10mM tris-HCl pH 8, 1mM PMSF, 1mM EDTA, 1% Formaldehyde) under vacuum (15 min at 25psi). The reaction was stopped adding 2M glycine and seedlings were filtered using Miracloth tissue and washed 3 times with milliQ water. Samples were ground in liquid Nitrogen to a fine powder, which was then added to extraction buffer 1 (0.4 M sucrose, 1m mM tris-HCl pH 8, 10 mM MgCl, 5mM ß-mercaptoethanol, 0.1mM PMSF, 10 μl/ml Protease Inhibitor Cocktail for plant cell and tissue extracts (Sigma Aldrich)). After filtering through Miracloth tissue, samples were centrifuged at 5,000 g for 20 min at 4 °C. The pellet was resuspended in 2 ml of Extraction Buffer 2 (0.25 M sucrose, 1% Triton X-100, and 10 μl/ml Protease Inhibitor Cocktail for plant cell and tissue extracts (Sigma Aldrich)) and precipitated by centrifugation at 12,000 g for 10 min at 4° C, and resuspended in 0.3 Extraction Buffer supplemented with 1.7 M sucrose, 0.15% Triton X-100, 2mM MgCl2, 5mM ß-mercaptoethanol, 0.1mM PMSF and 10 μl/ml Protease Inhibitor Cocktail for plant cell and tissue extracts, and centrifuged at 10,000 rpm for 1 h at 4°C. The resuspended solution was then layered on 0.3 ml of Extraction Buffer 3 and centrifuged for 1 hour at 16000 g at 4°C. The chromatin pellet was resuspended in 0.3 ml of Nuclei Lysis Buffer (50 mM Tris pH8.0, 10mM EDTA, 1% SDS, 0.1mM PMSF and 10 μl/ml Protease Inhibitor Cocktail for plant cell and tissue extracts) and sonicated to produce DNA fragments shorter than 500 bp. The sonicated suspension was centrifuged at 5,000 g for 5 min at 4°C, and supernatant was collected as a chromatin fraction. 70 μl of solution were removed to be used as Total DNA control. The remaining chromatin solution was further diluted in ChIP Dilution Buffer (1.1% Triton X-100, 1.2 mM EDTA, 16.7 mM Tris-HCl, 167 mM Nacl, 0.1mM PMSF, 10 μl/ml

Protease Inhibitor Cocktail for plant cell and tissue extracts) to a final volume of 3 ml. 0.1ml of the Chromatin solution was stored to be used as input control. The Protein A Agarose Dynabeads (Invitrogen) were incubated for 3 hours with 5 μl of anti-GFP antibody (ab290, Abcam) and washed three times in Chip Dilution Buffer. Then the Chromatin solution was incubated for 16 hours at 4°C with the beads. Beads were washed sequentially with the following buffers: Low Salt Wash buffer (150 mM NaCl, 0.1%SDS, 1% Triton X-100, 2 mM EDTA, 20mM Tris-HCl pH 8), High Salt Buffer (500 mM NaCl, 0.1%SDS, 1% Triton X-100, 2 mM EDTA, 20mM Tris-HCl pH 8), LiCl Buffer (0.25 mM LiCl, 1% NP40, 1% sodium deoxycholate, 1 mM EDTA, 10 mM Tris-HCl pH 8) and TE Buffer (10 mM Tris-HCl pH 8, 1 mM EDTA). The elution was done by incubating in 0.5 ml of Elution Buffer (0.1 M NaHCO3, 1% SDS) at 65 °C for 10 min twice and collecting the supernatant containing co-immunoprecipitated DNA. The co-immunoprecipitated chromatin and the input chromatin were decrosslinked by incubating for 16 hours with 5M NaCl at 65 °C. 10 μl of 0.5 M EDTA, 20 μl of Tris-HCl pH 6.5 and 2 μl of Proteinase K were added to the eluted DNA and placed for 1 hour at 45°C. DNA was purified by phenol-chloroform extraction and recovered by ethanol precipitation.

qRT-PCR on co-immunoprecipitated DNA fragments was performed as previously with the following primers:

qRTpIPT7-Afw catattcgtatatcaatggctggcc

qRTpIPT7-Arev cgtatatcaatggctggccatcaaactca

qRTpIPT7-Bfw ctgtatgtaagcatgcttgaa

qRTpIPT7-Brev gactttggtctacgaccttat

qRTpIPT7-Cfw tgacaactcacgactcgttgagg

qRTpIPT7-Crev cttgttcttgaagcacaagattgg

The fold enrichment of each fragment was obtained by normalizing the recovery rate for the *PHB*:GFP* preparation against that for the total input chromatin and was normalized to *OTC*. Experiments were performed in triplicates from three independent chromatin immunoprecipitations.

In Situ mRNA Hybridization

IPT7 in situ hybridization was performed as in SR10. The *IPT7* riboprobe was prepared from templates amplified from complementary DNA with the following primers:

atipt7utr3pf ttgatcatgtgaagctttttgg

atipt7utr3pr: tgatatcgtggcacaaggaa

ipt7probef caactacgattgttgtttcatttg

ipt7prober tcgcttggtctcgctacaag

PHB and *WUS* in situ hybridization was performed as in [10].

Computational Simulations (Related to Figure S4)

The observed regulatory interactions between CK, PHB and mir165/6 shown in Figure 4 form a feedforward loop [SR11], namely a network motif comprising three components in which the first component (CK) regulates the second component (mir165/5) such that both these components jointly regulate the third component (PHB). Using the terminology introduced in [SR12], the motif shown in Figure 4 is an example of an incoherent type 2 feedforward loop, with an additional feedback loop between the first and third components.

The simulations shown in Figure S4 A-C use a set of ordinary differential equations, which describe the evolution in concentrations of CK (C), PHB (P) and mir165/6 (M) as a result of the observed regulatory interactions. We use mass-action terms to describe both constitutive production of CK, PHB and mir/165/6, which occur at rates α_1, β_1 and γ_1, and natural degradation of these species, which occur at rates α_4, β_4 and γ_4. We model the direct interaction between PHB and mir165/6 similarly, with rate constant β_4. Hill-type kinetics are used to describe the regulation of transcription/synthesis of CK by PHB, of PHB by CK and of mir165/6 by CK, with maximum rates α_2, β_2 and γ_2 and half-saturation constants α_3, β_3 and γ_3 respectively. The equations for this model are therefore given by

$$\frac{dC}{dt} = \alpha_1 + \frac{\alpha_2 P^n}{\alpha_3^n + P^n} - \alpha_4 C,$$

$$\frac{dP}{dt} = \beta_1 + \frac{\beta_2}{1 + \left(\frac{C}{\beta_3}\right)^n} - (\beta_4 + \beta_5 M)P,$$

$$\frac{dM}{dt} = \gamma_1 + \frac{\gamma_2}{1 + \left(\frac{C}{\gamma_3}\right)^n} - \gamma_4 M.$$

We emphasize that these equations are not intended to capture the behaviour of the system in a quantitative manner, but rather as a simple model that allows us to investigate qualitatively how the combination of underlying interactions dictate the response of the system to a varying CK stimulus. A list of parameter values and definitions is provided in the following table.

Parameter	Definition	Numerical value
α_1	Baseline rate of CK synthesis	0 or 1
α_2	Maximum rate of PHB-induced CK synthesis	1
α_3	Apparent dissociation constant for PHB regulation of CK synthesis	0.5
α_4	Rate of CK degradation	1
β_1	Baseline rate of PHB transcription	1
β_2	Maximum rate of CK-inhibited PHB transcription	1
β_3	Dissociation constant for CK regulation of PHB transcription	0.4
β_4	Baseline rate of PHB degradation	1
β_5	Rate constant for mir165/6-induced PHB degradation	1
γ_1	Baseline rate of mir165/6 transcription	1
γ_2	Maximum rate of CK-inhibited mir165/6 transcription	1
γ_3	Dissociation constant for CK regulation of mir165/6 transcription	0.4
γ_4	Rate of mir165/6 degradation	1
N	Hill coefficient	1

This model is solved numerically using the Matlab ODE solver ode45, which implements a Runge-Kutta method with variable time step. To make a valid comparison, we compare the

results with a simpler model that lacks CK-inhibited mir165/6 transcription, and which has the same steady-state levels in the absence of constitutive CK synthesis ($\alpha_1 = 0$). More precisely, in this simpler model, we take $\gamma_3 = \infty$ to reflect the lack of CK inhibition of mir165/6 transcription and decrease γ_1 (to the value 0.4254) so as to obtain the same steady-state level of mir165/6 as in the full model.

We found that for the chosen parameter values, CK inhibition of mir165/6 transcription results in a dampened reduction, and accelerated recovery, of PHB in response to a temporary CK stimulus (simulated by increasing the constitute rate of CK synthesis, α_1, from 0 to 1 for a fixed duration). In order to establish the robustness of this model, we varied each parameter over two orders of magnitude (taking 100 values, from a tenth to ten times its reference value) while holding other parameter values constant. In each case we simulated the model and verified that the dampened reduction, and accelerated recovery, of PHB in response to a temporary CK stimulus was still observed.

Supplemental References

SR1. Mallory, A.C., Reinhart, B.J., Jones-Rhoades, M.W., Tang, G., Zamore, P.D., Barton, M.K. and Bartel, D.P. (2004). MicroRNA control of PHABULOSA in leaf development: importance of pairing to the microRNA 5' region. EMBO J. *23*, 3356-3364.

SR2. Clough, S.J. and Bent, A.F. (1998). Floral dip: a simplified method for Agrobacterium-mediated transformation of Arabidopsis thaliana. Plant J. *16*, 735–743.

SR3. Werner, T. Motyka, V., Laucou, V., Smets, R., Van Onckelen, H. and Schmülling, T. (2003). Cytokinin-Deficient Transgenic Arabidopsis Plants Show Multiple Developmental Alterations Indicating Opposite Functions of Cytokinins in the Regulation of Shoot and Root Meristem Activity. The Plant Cell *15*, 2532-2550.

SR4. Donnelly, P.M Bonetta, D., Tsukaya, H., Dengler, R.E. and Dengler, N.G. (1999). Cell cycling and cell enlargement in developing leaves of Arabidopsis. Dev. Biol. *215*, 407-419.

SR5. ten Hove, C.A., Willemsen, V., de Vries, W.J., van Dijken, A., Scheres, B. and Heidstra, R. (2010). SCHIZORIZA Encodes a Nuclear Factor Regulating Asymmetry of Stem Cell Divisions in the Arabidopsis Root. Curr. Biol. *20*, 452-457.

SR6. Hoffer, Pivashuta, S., Pontes, O., Vitins, A., Pikaard, C., Mroczka, A., Wagner, N. and Voelker, T. (2011). Posttranscriptional gene silencing in nuclei. Proc. Natl. Acad. Sci. U S A. *108*, 409–414.

SR7. Jasinski, S., Piazza, P., Craft, J., Hay, A., Woolley, L., Rieu, I., Phillips, A., Hedden, P. and Tsiantis**,** M. (2005). KNOX action in Arabidopsis is mediated by coordinate regulation of cytokinin and gibberellin activities. Curr. Biol. *15*, 1560-1565.

SR8. Nishiyama R., Watanabe, Y., Fujita, Y., Le, D.T., Kojima, M., Werner, T., Vankova, R., Yamaguchi-Shinozaki, K., Shinozaki, K., Kakimoto, T., Sakakibara, H., Schmülling, T. and Tran, L.S.(2011) Analysis of cytokinin mutants and regulation of cytokinin metabolic genes reveals important regulatory roles of cytokinins in drought, salt and abscisic acid responses, and abscisic acid biosynthesis. Plant Cell. *23* , 2169-2183

SR9. Saleh, A., Alvarez-Venegas, R and Avramova, Z. (2008). An efficient chromatin immunoprecipitation (ChIP) protocol for studying histone modifications in Arabidopsis plants. Nat. Protoc. *3*, 1018-1025.

SR10. Galinha, C., Hofhuis, H., Luijten, M, Willemsen, V., Blilou, I., Heidstra, R. and Scheres, B. (2007) PLETHORA proteins as dose-dependent master regulators of Arabidopsis root development. Nature.*449*, 1053-1057.

SR11. Shen-Orr, S., Milo, R., Mangan, S. and Alon, U. (2002). Network motifs in the transcriptional regulation network of Escherichia coli. Nat. Genet. *31*, 64-68.

SR12. Mangan, S. and Alon, U. (2003). Structure and function of the feed-forward loop network motif. Proc. Natl Acad. Sci. *100*, 11980-11985.

SR12. Mangan, S. and Alon, U. (2003). Structure and function of the feed-forward loop network motif. Proc. Natl Acad. Sci. *100*, 11980-11985.